

Dynamical simulation of transport in one-dimensional quantum wires

Kevin Leung,¹ Reinhold Egger,² and C.H. Mak¹

¹*Department of Chemistry, University of Southern California, Los Angeles, CA 90089-0482, USA*

²*Fakultät Physik, Albert-Ludwigs-Universität, Hermann-Herder-Straße 3, D-79104 Freiburg, Germany*

(Date: September 19, 1918)

Transport of single-channel spinless interacting fermions (Luttinger liquid) through a barrier has been studied by numerically exact quantum Monte Carlo methods. A novel stochastic integration over the real-time paths allows for direct computation of nonequilibrium conductance and noise properties. We have examined the low-temperature scaling of the conductance in the crossover region between a very weak and an almost insulating barrier.

PACS numbers: 72.10.-d, 73.40.Gk

Studies of transport in one-dimensional (1D) interacting Fermi systems have gathered novel physical insights and led to the development of several new techniques over the past few years. Instead of the usual Fermi liquid theory, the low-temperature properties of an idealized 1D quantum wire are described by the Luttinger liquid model [1,2]. Remarkable transport behaviors are expected for a Luttinger liquid in the presence of impurities or barriers, and several interesting theoretical [3–7] and experimental [8,9] studies have emerged recently. In this Letter, we describe a real-time quantum Monte Carlo (QMC) method that enables us to directly address the dynamics of a Luttinger liquid, and use it to investigate the low-temperature transport properties of a 1D quantum wire.

So far the only numerical approach to this problem has been the one given by Moon *et al.* [6]. These workers examined transport in a Luttinger liquid using Euclidean-time QMC simulations by analytically continuing numerical data to real time with Padé approximants. Mathematically, this analytic continuation is ill-posed and small statistical errors in the imaginary-time data could be magnified immensely [10]. Physically, imaginary-time data collected at low temperatures contain predominantly ground-state information whereas real-time dynamics is controlled by the excitation spectrum. Although the findings of Ref. [6] are certainly reasonable, a direct real-time simulation which avoids the possibly troublesome analytic continuation is desirable. Furthermore, a real-time simulation needs not rely on the Kubo formula and allows for direct computations of nonequilibrium transport and noise properties beyond the reach of previous methods.

Common to all real-time QMC simulations is the ubiquitous and fundamental *dynamical sign problem* [10–15]. It arises in the stochastic summation over the system

paths when the real-time propagators are oscillatory. The quantum-mechanical interference between different paths leads to a vanishing signal-to-noise ratio at very long real times and the simulation becomes effectively unstable. However, it is generally possible to treat intermediate-to-long times by employing a *partial summation scheme* [14] which reduces the effective number of variables subject to the Monte Carlo sampling. If guided by physical intuition, such a partial summation scheme can largely circumvent the dynamical sign problem. Previous applications to dissipative tight-binding models in the quantum-chemical context [14,15] have demonstrated the practical usefulness of this concept. Here, we adapt this idea to transport in interacting 1D quantum wires, and as we demonstrate below, the method is able to extract numerically exact results in the interesting low-temperature region.

Transport in Luttinger liquids depends crucially on a dimensionless parameter g which characterizes the electron-electron interaction strength. For the non-interacting case, $g = 1$. For $g < 1$, interactions are repulsive, and a barrier of any height leads to a perfect insulator at zero temperature. At asymptotically low temperatures, Kane and Fisher (KF) [3] have predicted the following scaling behavior for the linear dc conductance:

$$G \sim T^{2/g-2}. \quad (1)$$

Most analytical methods applied so far assume either a very small or a very large barrier height (impurity level) V_0 compared to the fermion bandwidth ω_c . For instance, perturbative arguments lead to Eq.(1) in the almost insulating case $V_0/\omega_c \gg 1$, while exact results [3–5,7] find the same scaling law for the opposite limit $V_0/\omega_c \ll 1$. Unfortunately, little is known in the crossover region between the two. A recent study [16] has shown that the usual bosonized impurity Hamiltonian [3] can be used to describe this crossover and is valid even for $\pi V_0/\omega_c > 1$, which corresponds to an impurity level outside the fermion band. Interestingly, Guinea *et al.* [17] have suggested a different low-temperature scaling form for the weak-barrier case

$$G = c_1 T^2 + c_2 T^{2/g-2}. \quad (2)$$

While exact results [3–5,7] give $c_1 = 0$ for both $V_0/\omega_c \gg 1$ and $V_0/\omega_c \ll 1$, they cannot rule out the T^2 scaling term for *intermediate* barrier heights $\pi V_0/\omega_c \approx 1$. A

naive reasoning leading to Eq.(2) for intermediate barriers is as follows. While the anomalous KF scaling exponents hold near the quantum critical points $V_0/\omega_c = 0$ and ∞ , scale invariance may not survive far away. One might then expect regular analytical behavior $G \sim T^n$ with even power n , and the lowest-order term would give T^2 as shown in (2). If this scaling form is indeed true, at sufficiently low temperatures the T^2 scaling would dominate for $g < 1/2$ and the KF law (1) could only be observed for $g > 1/2$. This prediction is clearly of practical importance for future experiments on quantum wires. As an application of our QMC method, we will address the validity of (2) here.

The action for the Luttinger liquid transport problem is usually formulated in terms of a phase field θ [2]. In the presence of a short-ranged impurity potential of effective strength (barrier height) V_0 , the (real-time) Lagrangian density takes the form [3]

$$\mathcal{L} = (1/2g) \partial_\mu \theta(x, t) \partial^\mu \theta(x, t) + V_0 \delta(x) \cos[2\sqrt{\pi}\theta(x, t)] + (eV/\sqrt{\pi}) \delta(x) \theta(x, t), \quad (3)$$

where V denotes an external static voltage. Since one can eliminate all degrees of freedom away from the barrier by Gaussian integrations, a naive real-time QMC simulation scheme would have to perform a stochastic summation over all possible $\theta(x=0, t)$ paths. After discretization of the time line, one is thus left with the task of sampling a high-dimensional integral where each of the integration variables $\theta(0, t_j)$ corresponding to time slice j is a c -number.

For numerical reasons, it is now advantageous to perform the real-time simulation within an equivalent discrete model (a “charge representation”). Discrete variables significantly reduce the relevant configuration space subject to Monte Carlo sampling compared to the θ variables which are continuous. Their use constitutes the first major step of our partial summation scheme. One can generally transform Luttinger liquid transport problems involving elastic scattering by short-ranged impurities into a discrete representation. This is achieved by expanding the impurity propagator [18],

$$\begin{aligned} & \exp \left[-iV_0 \int_0^t dt' \cos(2\sqrt{\pi}\theta(0, t')) \right] = \\ & \sum_{j=0}^{\infty} \int_0^t dt_j \int_0^{t_j} dt_{j-1} \cdots \int_0^{t_2} dt_1 (-iV_0/2)^j \\ & \times \sum_{\{q_j\}} \exp \left[2\sqrt{\pi}i \int_0^t dt' q_j(t') \theta(0, t') \right], \end{aligned} \quad (4)$$

where $q_j(t') = \sum_{i=1}^j \xi_i \delta(t' - t_i)$ is built from the discrete variables $\xi_i = \pm 1$.

The discrete “charges” ξ_i can be understood as Hubbard-Stratonovich fields. Introduction of these auxiliary fields permits us to perform the now Gaussian integration over the Luttinger liquid bosons θ . Naturally,

such mapping onto a discrete charge representation is not confined to Luttinger-liquid-type electron-electron interactions and can be done for any Coulomb interaction potential. Furthermore, one can use similar charge representations based on (4) for a multi-barrier problem, allowing for studies of resonant tunneling or related phenomena. In the following, we will focus on Eq.(3), which describes a Luttinger liquid impinging on a single barrier.

The nonlinear conductance $G(T, V) = \partial I / \partial V$ for transport of the Luttinger liquid through a barrier can be readily computed from the bosonized current operator, $J = (e/\sqrt{\pi}) \dot{\theta}(0)$. In fact, the conductance is

$$G(T, V) = (e/\sqrt{\pi}) (\partial/\partial V) \lim_{t \rightarrow \infty} \langle \dot{\theta}(0, t) \rangle, \quad (5)$$

where the average is taken using (3). In practice, the expectation value $\langle \dot{\theta}(0, t) \rangle$ reaches a plateau value after some time t^* , and if the real-time QMC scheme is able to reach this plateau, the conductance can be computed directly from the plateau value. Since t^* grows very large at extremely low temperatures, our method becomes increasingly costly near zero temperature. However, as shown below, the dynamical sign problem can be effectively circumvented to allow for studies in the interesting low-temperature scaling region.

Evaluating (5) by QMC requires construction of a discretized path-integral expression for $\langle \dot{\theta}(0, t) \rangle$, where t is the maximum length of the time line considered in the simulation. Eliminating all θ degrees of freedom away from the barrier, $\langle \dot{\theta}(0, t) \rangle$ is expressed as a weighted sum over all sets of forward-backward real-time paths $\{\theta_f(0, t'), \theta_b(0, t')\}$ with t' going from $t' = 0$ to t . In the next step, we switch to the charge representation using Eq.(4). One can then integrate out the $\theta(0)$ paths as well as at the price of introducing the auxiliary discrete charge paths $q_f(t')$ and $q_b(t')$. The resulting effective action contains nonlocal couplings between $\{q_f, q_b\}$ due to the eliminated θ modes.

Next we express q_f and q_b in terms of their symmetrized and antisymmetrized linear combinations. This constitutes the second major step with regard to the partial summation scheme. The symmetrized component corresponds to a quasiclassical degree of freedom since it describes propagation along the diagonal of the reduced density matrix. The antisymmetrized path, on the other hand, describes quantum fluctuations corresponding to the off-diagonal elements of the reduced density matrix.

The basic idea of the partial summation scheme is to split off part of the Monte Carlo problem to be evaluated non-stochastically, while leaving the remainder for the stochastic summation. This can be achieved by blocking states together in the course of the Metropolis walk: instead of sampling states individually, one non-stochastically probes the local surroundings of a given state to account for its degree of destructive interference [14]. Such a blocking strategy avoids regions with highly

destructive interference which do not contribute to the path integral in the first place but are responsible for the dynamical sign problem. In the present case, this strategy can be implemented very efficiently by noting that one can sum over all symmetrized components exactly. This is possible since there are no quasiclassical self-interactions in the effective action. In the end, only the antisymmetric paths are left for the Monte Carlo.

Any antisymmetric path can now be characterized by “kinks” y_i and the respective kink times t_i . In the QMC calculation, we have to discretize time into N sufficiently small slices of length $\delta t = t/N$, and no more than one kink is allowed on each time slice. The possible kink values are $y_i = 0, \pm 1, \pm 2$ corresponding to the charges $\xi = \pm 1$ of the original forward-backward charge paths. The Monte Carlo algorithm then performs a stochastic summation over all possible kink configurations $\{y\}$. We have used both kink migration and double kink flip moves to generate the Metropolis trajectory. The MC weight function is defined such that $\langle \dot{\theta}(0, t') \rangle$ is evaluated only at the endpoint $t' = t$. Our algorithm channels all efforts into generating relevant configurations at this one time point alone.

To check our QMC simulation scheme, we have carried out two independent tests: (a) short-time exact enumeration results are accurately reproduced, (b) additional QMC simulations for the static noise $\langle I^2 \rangle$ show that the familiar Johnson-Nyqvist formula is fulfilled at all temperatures. The results presented below employed discretizations on the order of $V_0 \delta t \approx 0.3$, and an upper time limit of $V_0 t = 20$ was sufficient to reach the plateau region of $\langle \dot{\theta}(0, t) \rangle$ for the temperatures studied here. Typically, numerical results for the low-temperature region were obtained using 25 to 250 million passes and our code performs at an average speed of 1 CPU hour per million passes on an IBM RISC 6000 Model 590.

Next we present numerical results for transport of a Luttinger liquid through a barrier. Figures 1 and 2 show simulation data for the linear conductance G at the two interaction strengths $g = 1/3$ and $g = 2/3$, respectively. We have studied two different barrier heights, $V_0/\omega_c = 1/6$ and $V_0/\omega_c = 1/3$. The value $g = 1/3$ is of direct relevance to tunneling of edge state excitations in the fractional quantum Hall effect [5,6,9], while recent transport experiments in quantum wires [8] have been carried out at $g = 0.67 \pm 0.03$. Our results are of immediate interest for these experiments.

The main panels show the QMC data over a wide range of temperatures. We compare our data to the thermodynamic Bethe ansatz solution by Fendley, Ludwig, and Saleur (FLS) [5] which is exact in the weak-barrier case $V_0/\omega_c \ll 1$. The Kondo temperature is defined as [5]

$$k_B T_B / V_0 = t_g (\pi V_0 / \omega_c)^{g/(1-g)},$$

with $t_{1/3} = 1.19599$ and $t_{2/3} = 0.80549$. The scaling variable used in the figures is

$$X = d_g (T_B / T)^{1-g},$$

where d_g is readily determined from the golden rule limit [3] (specifically, $d_{1/3} = 0.74313$ and $d_{2/3} = 0.99806$). The FLS solution reproduces the golden rule behavior

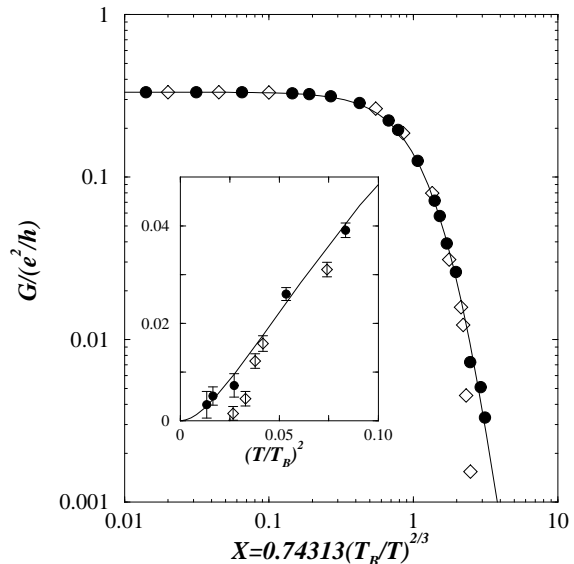


FIG. 1. QMC data for the linear conductance $G(X)$ at $g = 1/3$. Barrier heights are $V_0/\omega_c = 1/6$ (circles) and $V_0/\omega_c = 1/3$ (diamonds). The solid curve is the FLS solution [5]. Inset: Low-temperature behavior. Error bars denote one standard deviation, and the solid curve is again the FLS solution.

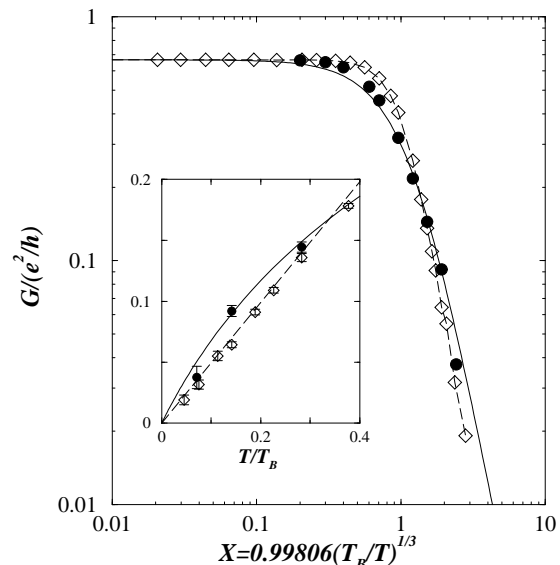


FIG. 2. QMC data for $G(X)$ at $g = 2/3$. Barrier heights are $V_0/\omega_c = 1/6$ (circles) and $V_0/\omega_c = 1/3$ (diamonds). The solid curve is the FLS solution, the dashed curve is a guide to the eye only. Inset: Low-temperature behavior.

$G/(e^2/h) = g(1 - X^2)$ at $T \gg T_B$ (small X), while for $T \ll T_B$ it matches the KF scaling law (1),

$$G(X)/(e^2/h) = K_g X^{-2/g} \quad (\text{large } X), \quad (6)$$

where $K_{1/3} = 3.3546$ and $K_{2/3} = 0.8177$.

For $g = 1/3$, we compare our numerical results with the FLS curve at two values of the barrier height, $V_0/\omega_c = 1/6$ and $1/3$ (see Fig. 1). For the smaller barrier, we reproduce the Bethe ansatz results well. This is quite remarkable since one might have expected more deviations from the FLS solution which assumes $V_0/\omega_c \ll 1$. In the FLS solution, the T^4 scaling region is found only at very low temperatures T/T_B below ≈ 0.15 . This is corroborated by our results which also indicate the *absence* of asymptotic T^2 contributions to the linear conductance. The low-temperature KF scaling (1) thus seems to hold even for the intermediate barrier heights studied here. Over the higher temperature range $0.15 < T/T_B < 0.4$, an *apparent* T^2 scaling is reached which, however, does not persist into the asymptotic low-temperature regime. In the case of the higher barrier, rather large deviations from the FLS solution are seen, especially at low temperatures. Remarkably, the experimental data in Ref. [9] exhibit the same qualitative deviations.

In Fig. 2, data are presented for $g = 2/3$ corresponding to the recent quantum wire experiments by Tarucha *et al.* [8]. Even for the intermediate barrier heights $V_0/\omega_c = 1/6$ and $1/3$ considered here, we observe the $G \sim T$ scaling (1). While our data fully reproduce the FLS curve for $V_0/\omega_c = 1/6$, there are significant deviations for a higher barrier. For $V_0/\omega_c = 1/3$, we find a smaller value $K_{2/3} = 0.477 \pm 0.005$ instead of the FLS value 0.8177, but the low-temperature KF scaling (6) still holds. The intermediate-barrier-height effects for $g = 2/3$ and $g = 1/3$ are qualitatively similar.

In conclusion, we have developed and applied real-time quantum Monte Carlo simulations to low-temperature transport of a Luttinger liquid through an arbitrarily high barrier. The close agreement of our data with thermodynamic Bethe ansatz results is rather remarkable since we have studied impurity levels near the fermion band edge. For $V_0/\omega_c = 1/6$, the FLS solution is completely reproduced, and only in the higher barrier $V_0/\omega_c = 1/3$ case are significant deviations observed. Recent speculations about possible T^2 contributions to the linear conductance for intermediate barrier height are determined by our calculations to be incorrect, and the low-temperature $T^{2/g-2}$ scaling is supported for the full crossover from a weak to an almost insulating barrier. We believe that the method presented here will be useful in future studies of nonequilibrium transport, noise properties, and resonant tunneling.

We wish to thank Paul Fendley for providing the Bethe ansatz curves and other valuable inputs. We have benefitted from discussions with H. Grabert, H. Saleur, M. Sassetti, and U. Weiss. This research is supported by NSF under grants CHE-9216221 and CHE-9257094, and by the Camille and Henry Dreyfus Foundation and the

Alfred P. Sloan Foundation. Computational resources have been furnished by the IBM Corporation.

-
- [1] J.M. Luttinger, J. Math. Phys. **4**, 1154 (1963); V.J. Emery, in *Highly conducting one-dimensional solids*, ed. by J.T. Devreese *et al.* (Plenum 1979).
 - [2] F.D.M. Haldane, Phys. Rev. Lett. **47**, 1840 (1981); J. Phys. C **14**, 2585 (1981).
 - [3] C.L. Kane and M.P.A. Fisher, Phys. Rev. Lett. **68**, 1220 (1992); Phys. Rev. B **46**, 15233 (1992).
 - [4] K.A. Matveev and L.I. Glazman, Phys. Rev. Lett. **70**, 990 (1993); K.A. Matveev, X. Yue, and L.I. Glazman, Phys. Rev. Lett. **71**, 3351 (1993).
 - [5] P. Fendley, A.W.W. Ludwig, and H. Saleur, Phys. Rev. Lett. **74**, 3005 (1995); preprint cond-mat/9503172.
 - [6] K. Moon, H. Yi, C.L. Kane, S.M. Girvin, and M.P.A. Fisher, Phys. Rev. Lett. **71**, 4381 (1993).
 - [7] R. Egger, M. Sassetti, and U. Weiss, Phys. Rev. B **52**, xxx (1995).
 - [8] S. Tarucha, T. Honda, and T. Saku, Sol. Stat. Comm. **94**, 413 (1995).
 - [9] F.P. Milliken, C.P. Umbach, and R.A. Webb, Sol. Stat. Comm. (in press).
 - [10] J.E. Gubernatis, M. Jarrell, R.N. Silver, D.S. Sivia, Phys. Rev. B **44**, 6011 (1991).
 - [11] A.P. Vinogradov and V.S. Filinov, Sov. Phys. Dokl. **26**, 1044 (1981); V.S. Filinov, Nucl. Phys. B **271**, 717 (1986).
 - [12] J.D. Doll, D.L. Freeman, and M.J. Gillan, Chem. Phys. Lett. **143**, 277 (1988); J.D. Doll, T.L. Beck, and D.L. Freeman, J. Chem. Phys. **89**, 5753 (1988).
 - [13] N. Makri and W.H. Miller, Chem. Phys. Lett. **139**, 10 (1987); N. Makri, Comp. Phys. Comm. **63**, 389 (1991).
 - [14] C.H. Mak, Phys. Rev. Lett. **68**, 899 (1992); R. Egger and C.H. Mak, Phys. Rev. B **50**, 15210 (1994).
 - [15] C.H. Mak and R. Egger, Phys. Rev. E **49**, 1997 (1994).
 - [16] R. Egger and H. Grabert, unpublished.
 - [17] F. Guinea, G. Gomez-Santos, M. Sassetti, and M. Ueda, preprint cond-mat/9411130.
 - [18] A. Schmid, Phys. Rev. Lett. **51**, 1506 (1983); M.P.A. Fisher and W. Zwerger, Phys. Rev. B **32**, 6190 (1985).